



Preparation, Characterization, *In vitro* Cell Cytotoxicity and Biological Studies of Pd(II), Ag(I), Pt(IV) and Hg(II) Piroxicam Anti-inflammatory Drug Complexes



Walaa H. El-Shwiniy^{a,b}, Mostafa Y. Nassar^c, A.M.A. Shehata^{a,d}, S. I. El-Desoky^c

^aDepartment of Chemistry, College of Science, University of Bisha, Bisha, 67714 Kingdom of Saudi Arabia

^bDepartment of Chemistry, Faculty of Science, Zagazig University, Zagazig 44519, Egypt

^cDepartment of Chemistry, Faculty of Science, Benha University, Benha 13518, Egypt

^dDepartment of Chemistry, Faculty of Science, Al Arish University, Al Arish, 45511 Egypt.

Abstract

Novel Pd(II), Ag(I), Pt(IV) and Hg(II) piroxicam (Pir) anti-inflammatory drug complexes were obtained upon the reaction of metal salts with piroxicam (Pir) in ethanol solvent at 60 °C. The proposed structure was explained with the aid of microanalytical analyses, conductivity, spectroscopic (FT-IR and UV-Vis.), magnetic calculations and thermogravimetric analyses (TG/TGA). The ratio of metal: Pir drug is found to be 1:2 in all complexes estimated by using molar ratio method. The conductance data reveal that Pd(II), Pt(II) and Hg(II) chelates are non-electrolytes except Ag(I) complex. The infrared spectrum of free piroxicam in comparison with its chelates indicated that the chelation mode occurs via the oxygen and nitrogen atoms of $\nu(\text{C}=\text{O})$ carbonyl and $\nu(\text{C}=\text{N})$ pyridyl, respectively. The kinetic parameters of thermogravimetric and its differential, such as activation energy, entropy of activation, enthalpy of activation, and Gibbs free energy were evaluated using Coats-Redfern and Horowitz-Metzger equations for Pir drug and its complexes. The antimicrobial tests were assessed toward some types of bacteria and fungi. The in-vitro cell cytotoxicity of the complexes in comparison with Pir against colon carcinoma (HCT-116) cell line was investigated.

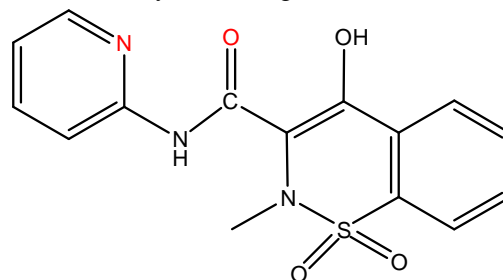
Keywords: Piroxicam (Pir); IR spectroscopy; Thermal analysis; Cytotoxicity.

1. Introduction

Piroxicam (Pir, 4-hydroxy-2-methyl-N-(pyridin-2-yl)-2H-benzo[e][1,2]thiazine-3-carboxamide 1,1-dioxide; Scheme 1) had been utilized as an operative anti-inflammatory drug [1]. Pir was a substantially delightful chemical structure of having four various heteroatom positions to be strong chelators for several metal ions [1-8].

The reality that metal ions perform remarkable roles in biological regulations had been uniquely determined. Metals were observed main to a human

body existence an entire bit of an organic frame in execute physiologically serious and vital functions in the body. The existence of the metallic ions can affect the bioavailability of the drug [1].



Scheme 1: The molecular structure of piroxicam.

*Corresponding author e-mail: whelmy@ub.edu.sa; walaa1986@zu.edu.eg; (W.H. El-Shwiniy).

Receive Date: 04 September 2019, Revise Date: 16 October 2019, Accept Date: 07 July 2020

DOI: 10.21608/EJCHEM.2019.16596.2011

©2020 National Information and Documentation Center (NIDOC)

It resembles that the role of metal ions is imperious for the path of function of piroxicam. The preparation and characterization of novel metal piroxicam complexes are important for preferable realization of the drug-metal interactions [1-9].

A detailed survey of literature reveals that, the preparation of the Pir metal complexes had been previously reported [1-13] and by checking it, We are going to study the synthesis and characterization of some Pir complexes with Pd(II), Ag(I), Pt(IV) and Hg(II) to determine the site of donation and the influence of atomic volume and oxidation state of the transition metal ions on microbial activity of Pir drug. All complexes were characterized by molar conductivities, melting point, magnetic properties, elemental analysis, infrared, ^1H NMR, mass, UV-Vis spectroscopy as well as thermal analysis. The antimicrobial activity of the tested complexes, metal salts, and free ligand (Pir) was tested against two Gram-positive *Staphylococcus aureus* (*S. aureus*), *Bacillus subtilis* (*B. subtilis*), and two Gram-negative bacteria species *Escherichia coli* (*E. coli*), *Pseudomonas aeruginosa* (*P. aeruginosa*), one fungal species *Candida albicans* (*C. albicans*). Also, the anti-tumor activity of the solid complexes was treated against a human colon carcinoma cell line (HCT-116 cells) was gained from American Type Tissue Culture Unit.

2. Experimental

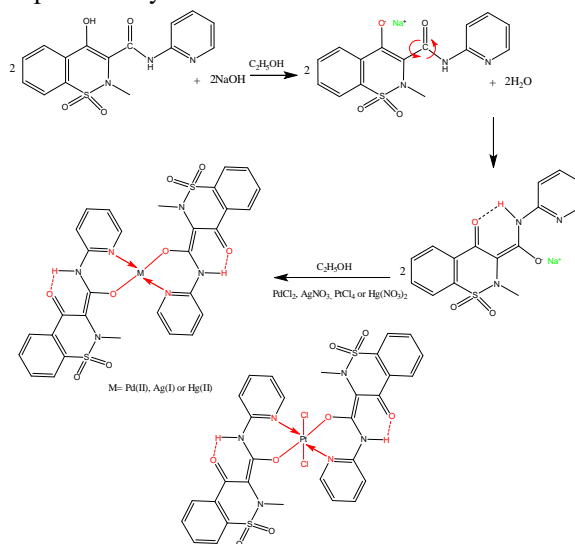
Materials

All chemicals used for the preparation of the complexes were of analytical reagent grade, commercially available from different sources, and used without further purification. Piroxicam was purchased from Medizen Pharmaceutical Industries, Egypt. AgNO_3 and $\text{Hg}(\text{NO}_3)_2$ were provided by Sigma-Aldrich Company. PdCl_2 , PtCl_4 and all solvents were purchased from Fluka Chemical Co.

2.1. Synthesis

An ethanolic solution (10 mL) of NaOH (1 mmol, 0.40 g) was added dropwise with stirring to a solution of piroxicam (1 mmol, 0.331 g) in ethanol (10 mL). To the piroxicam (Pir^-) solution, a hot ethanolic solution (60 °C, 10 mL) of PdCl_2 , AgNO_3 , PtCl_4 or $\text{Hg}(\text{NO}_3)_2$ (0.5 mmol, 0.177 g, 0.169 g, 0.336 g, 0.324 g) was then added and the mixture was refluxed for 3 h (Scheme 2). The complexes were precipitated as microcrystalline powders. They were

removed by filtration, washed with hot ethanol followed by diethylether and dried in a vacuum desiccator over anhydrous calcium chloride. All the complexes are colored and produced as powder. Their stoichiometries were confirmed by chemical analysis. The water content was confirmed, independently, by thermogravimetric analysis. The m.p. and analytical data are collected in Table 1.



Scheme 2: Synthesis route of piroxicam metal complexes.

2.2. Instrumentation-physical measurements

C, H and N analysis was carried out on a Perkin Elmer CHN 2400. The percentages of the metal ions were determined gravimetrically by transforming the solid products into metal oxide or ion. The percentages of the metal ions were also estimated using an atomic absorption spectrometer. The spectrometer model was PYE-UNICAM SP 1900 and fitted with the corresponding lamp. IR spectra were recorded on FT-IR 460 PLUS (KBr discs) in the range from $4000\text{--}400\text{ cm}^{-1}$. ^1H -NMR spectra were measured on Varian Mercury VX-300 NMR spectrometer using DMSO-d_6 as solvent. TGA-DTG measurements were carried out with heating rate of $20\text{ }^\circ\text{C min}^{-1}$ under N_2 atmosphere from room temperature to $800\text{ }^\circ\text{C}$ using TGA-50H Shimadzu. The mass of sample was accurately weighted out in an aluminum crucible. Absorbance measurements were conducted on a double beam spectrophotometer (T80 UV/Vis) with wavelength range $190\text{ nm} \sim 1100\text{ nm}$, spectral bandwidth of 2 nm . Mass spectra were recorded on GCMS-QP-2010 plus Shimadzu (ESI-

70ev) in the range from 0-1090. Magnetic measurements were carried out on a Sherwood scientific magnetic balance using Gouy balance using $\text{Hg}[\text{Co}(\text{SCN})_4]$ as calibrate. Melting points were determined using an Electrothermal- 9100 apparatus. Molar conductivities of the solutions of the ligand and metal complexes in DMSO with concentrations of 1×10^{-3} M were measured on CONSORT K410.

2.3. Screening for antimicrobial activity

The in-vitro antimicrobial activity of Pir ligand and its complexes towards the bacteria: two Gram-positive *Staphylococcus aureus* (*S. aureus*), *Bacillus subtilis* (*B. subtilis*), and two Gram-negative bacteria species *Escherichia coli* (*E. coli*), *Pseudomonas aeruginosa* (*P. aeruginosa*) in Mueller Hinton-Agar medium and fungi: *Candida albicans* (*C. albicans*) in Doxs medium were investigated. The antibacterial and antifungal activities were done at 20 mg/mL concentrations in DMSO solvent. Antimicrobial activity of the tested samples was determined using a modified Kirby-Bauer disc diffusion method [13] at general procedure for bacteria and fungi [14]. The microbial suspension was spread onto agar plates corresponding to the broth in which they were maintained. The bacterial strains; *S. aureus*, *B. subtilis*, *E. coli* and *P. aeruginosa* were incubated for 24 h at 37 °C and fungi strains; *C. albicans* was incubated at 30 °C for 48 h respectively, then the diameters of the inhibition zones were measured in millimeters. Blank paper discs (Schleicher & Schuell, Spain) with a diameter of 8.0 mm were impregnated 10 μL of tested concentration of the stock solutions. Standard antibacterial (Tetracycline) and antifungal drug (Amphotericin B) were used as references to evaluate the potency of the tested compounds under the same conditions. Activity was determined by measuring the diameter of the zone showing complete inhibition (mm). 10 μL of solvent (DMSO) were used as a negative control. Finally the activity results are calculated as a mean of triplicates.

2.4. Anticancer activity

Potential cytotoxicity of the isolated solid complexes was tested using the method of Skehan and Storeng [15]; cells were plated in 96-multiwell plate (104 cells/well) for 24 h before treatment with the complexes to allow attachment of cell to the wall of the plate. Different concentrations of the complexes under investigation (0, 5, 12.5, 25, 50 and 100 $\mu\text{g mL}^{-1}$) were added to the cell monolayer triplicate wells and were prepared for each individual dose. The monolayer cells were incubated with the complexes for 48 h at 37 °C and in 5 % CO_2 atmosphere. After 48 h, cells were fixed, washed and stained with SRB stain. Excess stain was washed with acetic acid and attached stain was recovered

with tris-EDTA buffer. The optical density (O.D.) of each well was measured spectrophotometrically at 564 nm with an ELISA microplate reader, and the mean background absorbance was automatically subtracted and mean values of each drug concentration was calculated. The relation between surviving fraction and drug concentration is plotted to get the survival curve of breast tumor cell line for each complex.

Calculation

The percentage of cell survival was calculated as follows:

Survival fraction = O.D. (treated cells) / O.D. (control cells).

The IC50 values (the concentrations of the Pir ligand or its complexes required to produce 50 % inhibition of cell growth) were calculated. The experiment was repeated three times for HCT-116 cell line.

3. Results and discussion

The microanalysis and spectroscopic measurements led to identify of new Pd(II), Ag(I), Pt(IV) and Hg(II) Pir complexes. The resulted complexes are colored powdered materials, constant in air, unsolvable in water and common solvents but they are soluble in DMSO and DMF. The molar conductance measurement was performed in DMSO solvent. Molar conductivities (Λ_m) of 1×10^{-3} M solutions of the ligand and complexes in DMSO are in the range of 10.0-53.30 $\text{S cm}^2 \text{mol}^{-1}$. The conductivity data refers that the non-electrolytic behavior for all complexes except Ag(I) is electrolyte [16,17]. The elemental analyses results of Pir complexes were near each other and are in the allowed range of $\pm 0.5\%$ error. The stoichiometry of the studied Pir chelates is determined by applying molar ratio method. Chemical analysis data and stoichiometry (Table 1) of the complexes indicated the formation of 1:2 [M:Pir] ratio and also all the synthesized complexes contained different numbers of water molecules. The elemental analysis was in good agreement with the chemical formulas of the complexes. The thermal analyses and infrared spectra data also prove the existence of water in the structure of Pd(II), Ag(I) and Hg(II) complexes. The magnetic moments (B.M.) of the complexes were measured at room temperature and all complexes were diamagnetic character.

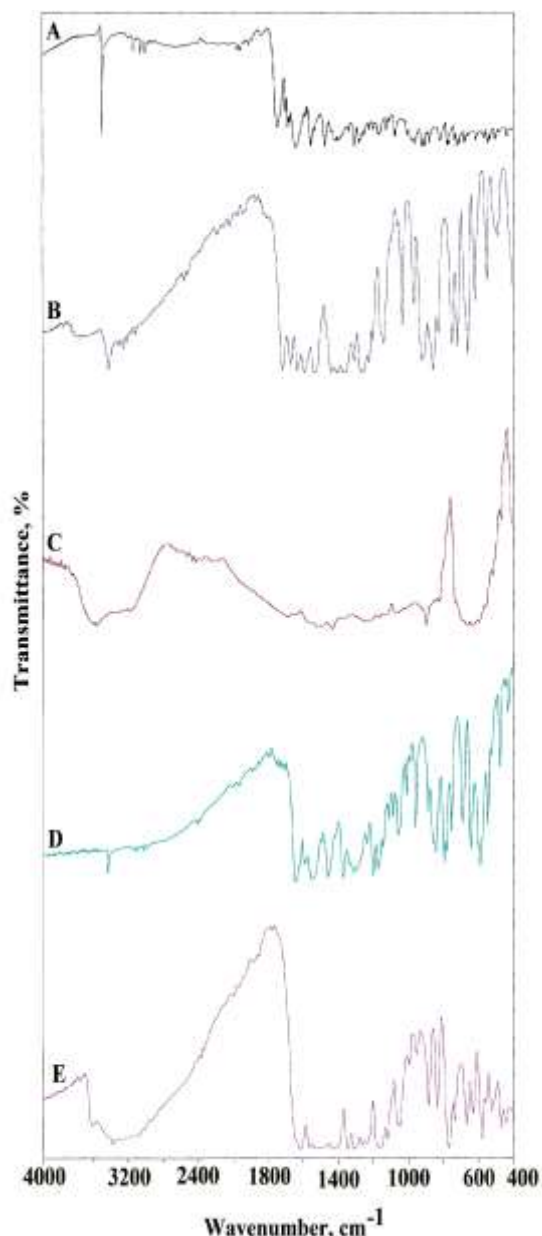


Fig. 1. Infrared spectra for (A) Pir, (B) $[\text{Pd}(\text{Pir})_2] \cdot \text{H}_2\text{O}$, (C) $\text{Na}[\text{Ag}(\text{Pir})_2] \cdot 3\text{H}_2\text{O}$, (D) $[\text{Pt}(\text{Pir})_2\text{Cl}_2]$, (E) $[\text{Hg}(\text{Pir})_2] \cdot 3\text{H}_2\text{O}$.

3.1. IR data and bonding

The FT-IR spectra of Pd(II), Ag(I), Pt(IV) and Hg(II) complexes contains the main absorption peaks of Pir free ligand (Table S1). The infrared spectra of the free Pir and its metal complexes were measured as KBr discs in the 4000-400 cm^{-1} range. These spectra are shown in Fig. 1 and the assignments are given in Table S1. There are several guide peaks in the ligand spectrum which their intensities or position expected to be shifted upon complexation, i.e., involved in chelation. The complexes IR spectra are extremely identical due

to the same atoms of ligand skeleton involved in the binding to the metal ions. In most instances, the suggested chelation mechanism of the Pir and metal ions interaction was by pyridine and amide groups; subsequently, we initial center our interest on these group vibrations. The infrared spectra of Pir complexes show a broad band between 3379 and 3464 cm^{-1} , assigned to the $\nu(\text{O-H})$ vibration and proves the existence of water molecules in all complexes [18,19]. The two peaks observed at 1641 and 1555 cm^{-1} in the spectrum of the free ligand have been corresponding to the stretching vibration of amide $\nu(\text{C=O})$ and the pyridine $\nu(\text{C=N})$ groups, respectively [1-6]. The shift of the two characteristic bands to a lower frequencies values at 1609, 1555 cm^{-1} for Pd(II), at 1630, 1520 cm^{-1} for Ag(I), at 1630, 1518 cm^{-1} for Pt(IV) and at 1600, 1524 cm^{-1} for Hg(II), supporting the participation of the amide and pyridine groups of Pir in the metal coordination [6, 20-23].

The spectra of the separated solid complexes show a set of peaks with various intensities which characteristics for $\nu(\text{M-N})$ and (M-O) [24]. The $\nu(\text{M-N})$ and (M-O) bands appeared at 567 and 455 cm^{-1} for Pd(II), at 583, 466 cm^{-1} for Ag(I), at 571, 455 cm^{-1} for Pt(IV) and at 576, 471 cm^{-1} for Hg(II) (Table S1) which are absent in the spectrum of the free Pir. This indicates the coordination of Pir through both (C=N) pyridine and (C=O) amide groups. Thus, it is concluded that Pir behaves as a bidentate ligand coordinated to the metal ions through amide -CO and pyridine-N.

3.2. UV-Vis spectra

The Pir free donor contains observable absorption bands within ultraviolet scale 200–400 nm. The electronic system was changed in the chelation between Pir and metal ions. The spectrum of Pir presents maximum absorption bands at 296, 330 and 408 nm (Fig. 2) assigned to $\pi-\pi^*$ and $n-\pi^*$ transitions, respectively. The absorption bands of Pd(II) and Pt(IV) complexes shifted to higher values and appearance of novel bands is due to complexation behavior. The appearance of new bands and the increase in the absorption bands upon coordination are probably attributed to an increase of electron density and mass of metal ions upon complexation by ligand. And, on the other hand, a decrease in the electron density on donor atoms (lone pair of electrons on oxygen and nitrogen donor atoms). The complexes of Pd(II), Ag(I), Pt(IV) and Hg(II) showed bands at 488, 496, 498 and 498 nm, respectively, which may be assigned to ligand–metal charge transfer. Besides, Pd(II), Ag(I), and Pt(IV) complexes exhibit a d-d transition bands at 550, 572, 558 nm, respectively [17].

Table 1 : Elemental analysis and Physico-analytical data for Pir. and its metal complexes

Compounds M.Wt. (M.F.)	Yield %	Mp/ °C	Color	Calcd. (Found (%))					A_m^2 (S cm ⁻¹)
				C	H	N	Cl	M	
Pir. 331.08, (C ₁₅ H ₁₃ N ₃ O ₄ S)	-	205	White	54.36 (54.83)	3.92 (3.89)	12.68 (12.54)	-	-	10.00
[Pd(C ₁₅ H ₁₂ N ₃ O ₄ S) ₂].H ₂ O 769.13, (PdC ₃₀ H ₂₆ N ₆ O ₈ S ₂)	70	280	Faint gray	46.73 (46.50)	3.66 (3.44)	10.90 (10.45)	-	13.80 (13.73)	10.70
Na[Ag(C ₁₅ H ₁₂ N ₃ O ₄ S) ₂].3H ₂ O 845.60, (NaAgC ₃₀ H ₃₀ N ₆ O ₁₁ S ₂)	85	>360	green	42.51 (42.42)	3.81 (3.60)	9.92 (9.89)	-	12.73 (12.61)	58.30
[Pt(C ₁₅ H ₁₂ N ₃ O ₄ S) ₂ Cl ₂] 926.68, (PtC ₃₀ H ₂₄ N ₆ O ₈ S ₂ Cl ₂)	95	245	Dark gray	38.80 (38.60)	2.82 (2.70)	9.05 (8.99)	7.64 (7.56)	21.01 (21.00)	15.60
[Hg(C ₁₅ H ₁₂ N ₃ O ₄ S) ₂].3H ₂ O 915.33, (HgC ₃₀ H ₃₀ N ₆ O ₁₁ S ₂)	90	260	Amber yellow	39.28 (39.19)	3.52 (3.33)	9.16 (9.08)	-	21.87 (21.74)	6.50

Table 2: 1H NMR spectra data (δ, ppm) of pir and its metal complexes

Assignments (δ,ppm)	Compounds		
	Pir.	Ag(I)-Pir	Pt(II)_Pir
δH; (s,2H,H ₂ O)	-	3.40	-
δH; (s,3H,-CH ₃)	2.51	2.34	2.43
δH; (d,2H,-CH)	2.86	2.86	2.88
δH; (1.benzene)	(d,2H)	7.86, 7.88	7.85, 7.90
	(t,2H)	7.26, 7.28	7.13, 7.24
δH; (2-Pyridine)	(d,2H)	8.39, 8.41	8.40, 8.45
	(t,2H)	7.97, 8.06	7.94, 8.05
δH; (s,1H,-CHOH)	5.17	-	-
δH; (s,1H,-NH)	10.52	10.51	10.52

Table 3: Maximum temperature Tmax (°C) and weight loss values of the decomposition stages for Pir and Pd(II), Ag(I), Pt(IV) and Hg(II) complexes.

Compounds	Decomposition	T _{max} (°C)	Weight loss (%)		Assignment	
			Calc.	Found		
Pir (C ₁₅ H ₁₃ N ₃ O ₄ S)	First step	276, 605, 674	99.99	99.66	5C ₂ H ₂ +3HCN +2CO+SO ₂	
	Total loss		99.99	99.66		
	Residue		-	-		
[Pd(Pir) ₂].H ₂ O	First step	123	2.26	2.06	H ₂ O	
	Second step		292,503,646	83.82	83.39	12C ₂ H ₂ +6CO+N ₂ O+2N ₂ +S ₂ O
	Total loss		86.08	85.45		
	Residue		13.83	13.78	Pd	
Na[Ag(Pir) ₂].3H ₂ O	First step	82	6.38	5.97	3H ₂ O	
	Second step		139, 340, 811	73.55	73.03	12C ₂ H ₂ +S ₂ O+4NO+N ₂ O+2CO
	Total loss		79.94	79.00		
	Residue		21.06	21.00	Ag+Na+4C	
[Pt(Pir) ₂ Cl ₂]	First step	263,457,599	78.94	78.66	12C ₂ H ₂ +6CO+N ₂ O+2N ₂ +Cl ₂ +S ₂	
	Total loss		78.94	78.66		
	Residue		21.05	21.00	O	
[Hg(Pir) ₂].3H ₂ O	First step	90	5.89	5.65	Pt	
	Second step		148, 256, 684	72.18	72.00	3H ₂ O
	Total loss		78.07	77.65	13C ₂ H ₂ +4CO+NO ₂ +3N ₂ O+2SO	
	Residue		21.64	21.10	Hg	

Table 4: Thermal behavior and Kinetic parameters determined using Coats–Redfern (CR) and Horowitz–Metzger (HM) operated for Pir and its metal complexes.

compounds	T_s (K)	method	parameter					R^a	SD^b
			E^* (KJ/mol)	A (s^{-1})	ΔS^* (KJ/mol.K)	ΔH^* (KJ/mol)	ΔG^* (KJ/mol)		
Pir	549	CR	89.92	19.69×10^{-6}	-0.104	87.62	116.50	0.92	0.24
		HM	31.11	18.54×10^{-4}	-0.143	28.81	68.39	0.96	0.24
[Pd(Pir) ₂ Cl ₂].H ₂ O	565	CR	61.55	2.29×10^{-2}	-0.199	59.12	117.38	0.94	0.30
		HM	91.26	2.69	-0.236	66.98	75.75	0.95	0.14
[Ag(Pir) ₂]NO ₃ .3H ₂ O	613	CR	8.86	13.95×10^{-2}	-0.262	6.03	95.24	0.94	0.23
		HM	7.12	45.64×10^{-2}	-0.252	4.30	90.19	0.90	0.25
[Pt(Pir) ₂ Cl ₂]Cl ₂	536	CR	115.33	1.79×10^{10}	-0.199	193.16	190.97	0.96	0.11
		HM	195.34	1.04×10^{10}	-0.120	59.12	117.38	0.94	0.30
[Hg(Pir) ₂]NO ₃ .3H ₂ O	529	CR	45.67	3.52×10^{-3}	-0.175	2.43	47.42	0.99	0.13
		HM	13.30	0.6110^{-2}	-0.209	11.17	64.76	0.94	0.19

Table 5: Antibacterial and antifungal activities of Pir and its synthesized complexes

Compounds	Microorganisms				
	Fungi	Gram-positive Bacteria		Gram-negative Bacteria	
	<i>C. albicans</i> (RCMB005002)	<i>S. aureus</i> (RCMB000106)	<i>B. subtilis</i> (RCMB 000107)	<i>P. aeruginosa</i> (RCMB 000102)	<i>E. coli</i> (RCMB 000103)
Pir	3±0.09	10.00±0.08	7.00±0.60	4±0.07	8±0.04
Pd(II) – Pir	10 ⁺¹ ±0.08	18.8 ⁺¹ ±0.58	14.9 ⁺¹ ±0.06	20.3 ⁺² ±0.03	5.00 ^{NS} ±0.45
Ag(I)- Pir	12 ⁺¹ ±0.08	11.7 ^{NS} ±0.36	7.1 ^{NS} ±0.72	6 ^{NS} ±0.08	12.6 ⁺¹ ±0.57
Pt(IV)- Pir	20 ⁺² ±0.08	22.4 ⁺² ±0.03	29.1 ⁺⁵ ±0.08	24.1 ⁺⁵ ±0.04	17.4 ⁺² ±0.04
Hg(I) – Pir	11 ⁺¹ ±0.08	19.9 ⁺¹ ±0.03	15.2 ⁺¹ ±0.08	5 ^{NS} ±0.09	12.2 ⁺¹ ±0.2
Standard Tetracycline	-	12±0.07	9±0.1	5±0.09	7±0.04
Amphotericin B	11±0.08	-	-	-	-

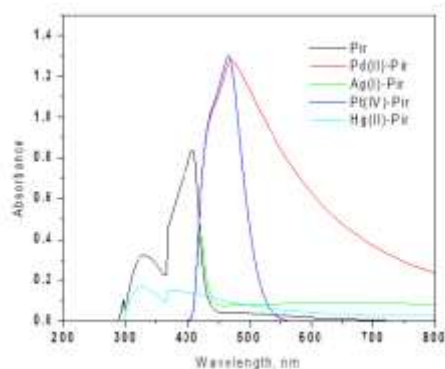


Fig. 2. Electronic absorption spectra of Pir and its metal complexes.

3.3. ¹H NMR spectral studies

The bonding mode of Pir was also confirmed by the ¹H NMR spectra of Pir ligand and its diamagnetic Ag(I) and Pt(IV) complexes. The ¹H NMR spectra of the complexes were recorded in DMSO-d₆ at room temperature using tetramethylsilane (TMS) as internal standard. The various kinds of proton chemical shifts in the ¹H NMR spectra of Pir ligand and its Ag(I) and Pt(IV) complexes are tabulated in Table 2. ¹H NMR spectrum of the ligand, Fig. S1, revealed a singlet signal at $\delta = 5.17$ ppm (s, 1H, -CHOH), $\delta = 10.52$ ppm (s, 1H, -NH) which was disappeared on addition of the D₂O [25]. A inspection of ¹H NMR spectra of diamagnetic Ag(I)

and Pt(IV) complexes with Pir ligand (Table 2) revealed the disappearance of chemical shift of the OH proton in the two complexes spectra. And this indicated the deprotonation of the hydroxyl group of the Pir upon coordination with Ag(I) and Pt(IV) confirming the bonding of oxygen to the metal ions [1-6]. It is found that all signals of Pir ligand observed in the spectra of complexes except at $\delta = 3.40$ ppm for Ag(I) complex can probably assigned to hydrated H₂O protons [24].

3.4. Thermal studies

The characterization of both organic and inorganic compounds performed by the most commonly used thermal analysis techniques (thermogravimetry, TG). Representative thermogravimetric figures are shown in Fig. 3. The maximum temperature values, $T_{max}/^{\circ}C$, together with the corresponding weight loss for each stage of degradation of the ligand and its complexes together with theoretical percentage mass losses are listed in Table 3.

The thermal decomposition for the ligand (Pir) begins at 25 °C and finished at 1000 °C with one main step. The decomposition takes place at three maxima 276, 605 and 674 °C and is totally accompanied by a weight loss of 99.66%, corresponding to loss of $5C_2H_2+3HCN+2CO+SO_2$, close to the calculated value 99.99%. $[Pd(Pir)_2].H_2O$ complex decomposed in two degradation steps, the first one occurs at maximum 123 °C and is accompanied by a weight loss of 2.06% corresponding to loss of H₂O molecule. The second step occurs at various temperatures and is accompanied by a weight loss of 83.39%, agrees with the theoretical value of 83.82% and the activation energy $61.55 \text{ KJ mol}^{-1}$.

The hydrated Ag(I) complex loses upon heating three water molecules in the first step at 82 °C. The second stage decomposed at three maxima at 139, 340 and 811 °C and accompanied by a weight loss of 75.10% leaving $Ag+4C$ as a final product and the activation energy 8.86 KJ mol^{-1} . The percentage for the residue after decomposition is 18.28% giving an actual total weight loss of 81.07% in agreement with our calculated total weight loss value of 81.55%. The $[Pt(Pir)_2Cl_2]$ exhibits one main decomposition step with three maxima at 263, 457 and 599 °C accompanied by weight loss of 78.66% corresponds to loss of $12C_2H_2+6CO+N_2O+2N_2+Cl_2+S_2O$, giving Pt as a final product with an activation energy $115.33 \text{ KJ mol}^{-1}$. The hydrated Hg(II) complex loses upon heating all water molecules at one maximum 90 °C.

The dehydrated Hg(II) piroxicam complex is simultaneously decomposed to Hg at various temperatures (Table 3) with intermediate formation of very unstable products which were not identified [26].

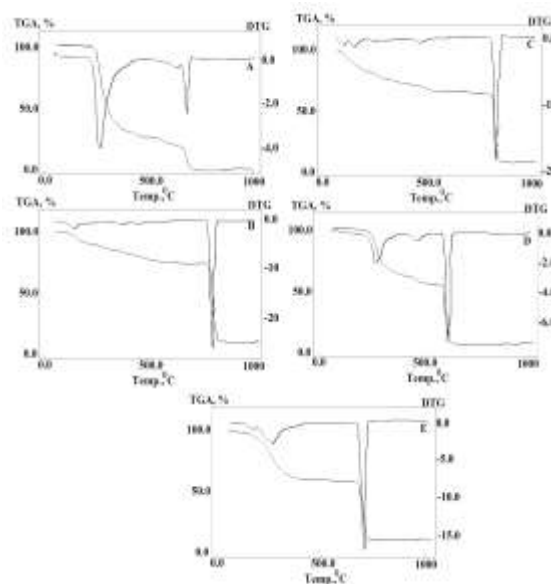


Fig. 3. TGA and DTG diagrams for (A) Pir, (B) $[Pd(Pir)_2].H_2O$, (C) $Na[Ag(Pir)_2].3H_2O$, (D) $[Pt(Pir)_2Cl_2]$, (E) $[Hg(Pir)_2].3H_2O$.

3.5. Kinetic data

The kinetic thermodynamic parameters such as activation energies, E^* , enthalpies, ΔH^* , entropies, ΔS^* and Gibbs free energies, ΔG^* , of the decomposition were evaluated graphically by employing the Coats-Redfern (CR) relationship [27]:

$$\ln \left[\frac{-\ln(1-\alpha)}{T^2} \right] = \frac{-E^*}{RT} + \ln \left[\frac{AR}{\phi E^*} \right]$$

Where α and ϕ are the fraction of the sample decomposed at time t and the linear heating rate, respectively. R is the gas constant and E^* is the energy of activation in kJ mol^{-1} and calculated from the slope and A in (s^{-1}) from the intercept. A plot of left-hand side (LHS) against $1/T$ was drawn using origin 6.0 program and the fit line is produced (Fig. S2). With information of R , A and ϕ , the enthalpy of activation, ΔH^* , and Gibbs free energy, ΔG^* , the entropy of activation ΔS^* in $(\text{J K}^{-1}\text{mol}^{-1})$, were calculated (Table 4) via the equations:

$$\Delta H^* = E^* - RT$$

$$\Delta G^* = \Delta H^* - T\Delta S^*$$

$$\Delta S^* = R \ln \left(\frac{Ah}{K_B T_e} \right)$$

Where KB is the Boltzmann constant, h is the Plank's constant and T_s is the DTG peak temperature [28].

and Horowitz-Metzger (HM) relationship [29]:

$$\log \left[\log \left(\frac{w_\infty}{w_t} \right) \right] = \frac{E^* \theta}{2.303RT_s^2} - \log 2.303$$

Where $\theta = T - T_s$, $w_\infty = w_\infty - w$, w_∞ = mass loss at the completion of the reaction; w = mass loss up to time t . The plot of $\log[\log(w_\infty/w_t)]$ versus θ was drawn and found to be linear from the slope of which E^* was calculated. The pre-exponential factor, A , was calculated from the equation:

$$\frac{E^* \theta}{RT_s^2} = \frac{A}{\left[\phi \exp \left(-\frac{E^*}{RT_s} \right) \right]}$$

The kinetic parameters were evaluated using the above mentioned methods by graphical means and they are listed in Table 4. The activation energies of decomposition were found to be in the range 7.12-195.34 kJ mol⁻¹. The high values of the activation energies reflect the thermal stability of the complexes. The entropy of activation was found to have negative values in all complexes which indicate that the decomposition reactions proceeded with a lower rate than the normal ones and activated complexes have more ordered systems than reactants.

4. Biological activities

The microbial studies proposed that, the isolated solid complexes were found to be biologically active and showed remarkable significantly antibacterial and antifungal (Table 5). The bacterial and fungi growth inhibitory capacities of the ligand and its complexes follow the order: Pt(IV) > Hg(II) > Pd(II) > Tetracycline > Ag(I) > Pir (for *B. Subtilis*), Pt(IV) > Hg(II) > Pd(II) > Tetracycline > Ag(I) > Pir (for *S. aureus*), Pt(IV) > Ag(I) > Hg(II) > Pir > Tetracycline > Pd(II) (for *E. coli*), Pt(IV) > Pd(II) > Ag(I) > Hg(II) > Tetracycline > Pir (for *P. aeruginosa*), Pt(IV) > Ag(I) > Hg(II) = Amphotericin B > Pd(II) > Pir (for *C. albicans*). The mechanism for the increase in antimicrobial activities may be considered in light of Overton's concept [30] and Tweedy's chelation theory [31]. Coordination reduces the polarity of the metal ion mainly because of the partial sharing of its positive charge with the donor groups [32, 33] within the chelate ring system formed during coordination. This process, in turn, increases the lipophilic nature of the central metal atom, which favors its permeation more efficiently through the lipid layer of the micro-organism [34-36] thus destroying them more aggressively.

4.1. Cytotoxic activity

The cytotoxicity assays of piroxicam and its complexes against tumor cell line (HCT-116) was evaluated; the IC₅₀ values derived from the experimental data were summarized in Table 6. From the results, it was notable that Pir free ligand was almost active against colon carcinoma cell line (HCT-116) with IC₅₀ values of 7.32 µg/ml. The tested compounds showed a remarkable antitumor activity and cytotoxic specificity toward human colon carcinoma cell line (HCT-116). Moreover, Ag(I) complex exhibited a higher antitumor activity than other complexes did on colonic cell line with IC₅₀ value 4.07 µg/ml (Fig. 4). The Pd(II) complex was less active than the free ligand against the carcinoma cell line tested.

Table 6.

The in vitro inhibitory activity of Pir and its metal complexes against tumor cell lines expressed as IC₅₀ values (µg/ml) ± standard deviation from six replicates.

Tested compounds	Tumor cell line	
	HCT-116	S.D. (±)
Pir	7.32	0.9
Pd(II)-(Pir) ₂	83.4	0.66
Ag(I)-(Pir) ₂	4.07	0.41
Pt(IV)-(Pir) ₂	17.5	0.53
Hg(II)-(Pir) ₂	11.4	0.68
Doxorubicin standard	0.46	0.1
5-Fluorouracil standard	4.3	0.2

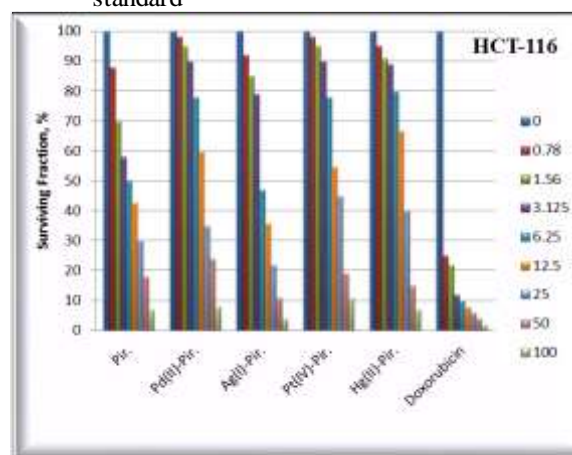


Fig. 4. The dose response curve showing the in vitro inhibitory activity of Pir and its metal complexes against human colon carcinoma (HCT-116) cell line.

5. Conclusion

The preparation and characterization of four complexes of piroxicam anti-inflammatory drug with Pd(II), Ag(I), Pt(IV) and Hg(II) have been achieved with physicochemical and spectroscopic methods. In the resultant complexes, Pir is bound to metal ions via the oxygen and nitrogen atoms of $\nu(\text{C}=\text{O})$ carbonyl and $\nu(\text{C}=\text{N})$ pyridyl. The kinetic parameters of thermogravimetric and its differential were evaluated using Coats-Redfern and Horowitz-Metzger equations for Pir drug and its complexes. The metal complexes exhibits higher inhibition against all microorganisms tested as well as Ag(I) complex exhibited a higher antitumor activity than other complexes compared to free Pir.

6. Conflicts of interest

“There are no conflicts to declare”.

7. Acknowledgments

The authors gratefully acknowledge to Zagazig University, Egypt and University of Bisha, Kingdom of Saudi Arabia for the support of this research work.

8. References

- [1] N.E.A. El-Gamel, Uranyl binary and ternary chelates of tenoxicam Synthesis, spectroscopic and thermal characterization of ternary chelates of tenoxicam and alanine with transition metals, *Spectrochim. Acta A*, 2007, 68, 860. <https://doi.org/10.1016/j.saa.2006.12.071>
- [2] J.E. Weder, C.T. Dillon, T.W. Hambley, B.J. Kennedy, P.A. Lay, J.R. Biffin, H.L. Regtop, N.M. Davies, Copper complexes of nonsteroidal anti-inflammatory drugs: An Opportunity yet to be realized, *Coord. Chem. Rev.* 2002, 232, 95. [https://doi.org/10.1016/S0010-8545\(02\)00086-3](https://doi.org/10.1016/S0010-8545(02)00086-3)
- [3] W.H. El-Shwiniy, W.S. Shehab, W.A. Zordok, Spectral, thermal, DFT calculations, anticancer and antimicrobial studies for bivalent manganese complexes of pyrano [2,3-d]pyrimidine derivatives, *J. Mol. Struct.*, 2020, 1199, 126993. <https://doi.org/10.1016/j.molstruc.2019.126993>
- [4] G.M. Gehad, E.A E-G. Nadia, Preparation and spectroscopic characterisation of metal complexes of piroxicam, *Vibrational Spectroscopy*, 2004, 36, 97. [doi:10.1016/j.vibspec.2004.04.004](https://doi.org/10.1016/j.vibspec.2004.04.004)
- [5] S.M. Abd El-Hamid, S.A. Sadeek, W.A. Zordok, W.H. El-Shwiniy, Synthesis, spectroscopic studies, DFT calculations, cytotoxicity and antimicrobial activity of some metal complexes with ofloxacin and 2,2-bipyridine, *J. Mol. Struct.* 2019, 1176, 422. <https://doi.org/10.1016/j.molstruc.2018.08.082>
- [6] H. Hadadzadeh, H. Farrokhpour, Z. Jannesari, Z. Amirghofran, Experimental and ONIOM computational evaluation of DNA- and BSA-binding and cytotoxic activity of a mononuclear Pd(II) complex with piroxicam, *Inorg. Chim. Acta*, 2016, 453, 415. <https://doi.org/10.1016/j.ica.2016.08.051>
- [7] S. Goswami, S. Sanyal, P. Chakraborty, C. Das, M. Sarkar, Interaction of a common painkiller piroxicam and copper-piroxicam with chromatin causes structural alterations accompanied by modulation at the epigenomic/genomic level *Biochim. et Biophys. Acta (BBA)-Gen.Subj.* 2017, 1861, 2048. [doi: 10.1016/j.bbagen.2017.04.006](https://doi.org/10.1016/j.bbagen.2017.04.006)
- [8] P. Christofis, M. Katsarou, A. Papakyriakou, Y. Sanakis, N. Katsaros, G. Psomas, Mononuclear metal complexes with Piroxicam: Synthesis, structure and biological activity, *J. of Inorg. Biochem.* 2005, 99, 2197. [doi:10.1016/j.jinorgbio.2005.07.020](https://doi.org/10.1016/j.jinorgbio.2005.07.020)
- [9] S.S. Wesam, W.H. El- Shwiniy, Nanoparticles of manganese oxides as efficient catalyst for the synthesis of pyrano[2,3- d]pyrimidine derivatives and their complexes as potent protease inhibitors *J. Iran. Chem. Soc.* 2018, 15, 431. <https://doi.org/10.1007/s13738-017-1244-4>
- [10] R. Cini, G. Giorgi, A. Cinquantini, C. Rossi, M. Sabat, The organotin(IV) coordination polymer [(Me3Sn)4Fe(CN)6.2H2O.C4H8O2].infin.: a three-dimensional host-guest network involving "cascade type" guests *Inorg. Chem.* 1990, 29, 5197. <https://doi.org/10.1021/ic00334a001>
- [11] E. Santi, M.H. Torre, E. Kremer, S.B. Etcheverry, E.J. Baran, Vibrational spectra of the copper(II) and nickel(II) complexes of piroxicam, *Vibration Spectroscopic*, 1993, 5, 285. [https://doi.org/10.1016/0924-2031\(93\)87004-D](https://doi.org/10.1016/0924-2031(93)87004-D)
- [12] S. El-Khateeb, S. Abdel Fattah, S. Abdel Razeg, M. Tawakkol, *Anal. Lett.* 1989, 22, 101. Analysis of Piroxicam Via Its Copper (Ii) and Iron (Iii) Complexes, A.W. Bauer, W.M. Kirby, J.C. Sherris, M. Turck, *Am. J. Clin. Pathol.* 1966, 45, 493. <https://doi.org/10.1080/00032718908051188>
- [13] M.A. Pfaller, L. Burmeister, M.A. Bartlett, M.G. Rinaldi, Multicenter evaluation of four methods of yeast inoculum preparation. *J. Clin. Microbiol.* 1988, 26, 1437. [https://doi.org/0095-1137/88/081437-05\\$02.00/0](https://doi.org/0095-1137/88/081437-05$02.00/0)
- [14] P. Skehan, R. Storeng, New Colorimetric Cytotoxicity Assay for Anticancer-Drug Screening, *J Natl Cancer Inst.* 1990, 82, 1107. <https://doi.org/10.1093/jnci/82.13.1107>
- [15] W.J. Geary, The use of conductivity measurements in organic solvents for the characterisation of coordination compounds, *Coord. Chem. Rev.* 1971, 7, 81. [https://doi.org/10.1016/S0010-8545\(00\)80009-0](https://doi.org/10.1016/S0010-8545(00)80009-0)
- [16] W.H. El- Shwiniy, W. S. Shehab, S. F. Mohamed, H. G. Ibrahim, Synthesis and cytotoxic evaluation of some substituted pyrazole zirconium (IV) complexes and their biological assay *Appl Organometal Chem.* 2018, 32, e4503. <https://doi.org/10.1002/aoc.4503>
- [17] E.K. Efthimiadou, A. Karaliota and G. Pasomas, Structure, antimicrobial activity and DNA-binding properties of the cobalt(II)-sparfloxacin complex, *Bio. org. Med. Chem. Lett.* 2008, 18, 4033. <https://doi.org/10.1016/j.bmcl.2008.05.115>
- [18] W.H. El-Shwiniy, S.A. Sadeek, Synthesis and characterization of new 2-cyano-2-(p-tolyl-hydrazono)-thioacetamide metal complexes and a study on their antimicrobial activities, *Spectrochim. Acta A*, 2015, 137, 535. <http://dx.doi.org/10.1016/j.saa.2014.08.124>
- [19] G.G. Mohamed, F.A. Nour El-Dien, N.E.A. El-Gamel, Synthesis, spectral and thermal studies of Mn(II), Co(II), Ni(II), Cu(II) and Zn(II) complex dyes based on hydroxyquinoline moiety, *J Therm Anal Calorim.* 2000, 67, 135. DOI: 10.1007/s10973-011-1911-0
- [20] E.Q. Castro, S. Berenes, N.B. Behrens, A.T. Behrens, A.T. Benavides, R. Contreras, H. Noth, Structural and spectroscopic characterisation of tris(2-benzimidazolylmethyl)amine coordination compounds of Zn(II), Cd(II) and Hg(II), *Polyhedron*, 2000, 19, 1479. [https://doi.org/10.1016/S0277-5387\(00\)00406-X](https://doi.org/10.1016/S0277-5387(00)00406-X)
- [21] W.R. Paryzek, E. Luks, The dioxouranium(VI) ion as a template for the synthesis of hexaaza tetradentate macrocyclic ligand, *Polyhedron*, 1994, 13, 899. [https://doi.org/10.1016/S0277-5387\(00\)83007-7](https://doi.org/10.1016/S0277-5387(00)83007-7)

- [22] K. Nakamoto, *Infrared and Raman Spectra of Inorganic and Coordination Compounds*, Wiley, New York, fourth ed., 1980.
- [23] S.A. Sadeek, S.M. Abd El-Hamid, W.H. El-Shwiniy, Synthesis, spectroscopic characterization, thermal stability and biological studies of mixed ligand complexes of gemifloxacin drug and 2,20-bipyridine with some transition metals, *Res Chem Intern.* 2016, 42, 3183. DOI 10.1007/s11164-015-2205-0
- [24] W.A., Zordok, Synthesis, spectroscopic, structural characterization, thermal analysis, kinetics, biological evaluation of non-steroidal anti-inflammatory drug diclofenac zirconium (IV) solvates (L) (L = H₂O, DMF, Py and Et₃N), *J. Mol. Struct.*, 1166, 270 (2018).
- [25] Ruiz M., Perellò L., Ortiz R., Castiñeiras A., Maichle-Mösser C. and Cantòn E., Synthesis, characterization, and crystal structure of [Cu(cinoxacinate)₂]. 2H₂O complex: A square-planar CuO₄ chromophore. Antibacterial studies, *J. Inorg. Biochem.* 1995, 801, 59.
- [26] A.W. Coats, J.P. Redfern, Kinetic Parameters from Thermogravimetric Data, *Nature*, 1964, 201, 68. <http://dx.doi.org/10.1038/201068a0>
- [27] P. Kofstad, Oxidation of Metals: Determination of Activation Energies, *Nature*, 1957, 179, 1362. doi 10.1038/1791362a0
- [28] H.W. Horowitz, G. Metzger, A New Analysis of Thermogravimetric Traces., *Anal. Chem.* 1963, 35, 1464. <https://doi.org/10.1021/ac60203a013>
- [29] U.K., Komamicka Starosta R., Kyzioł A., Płotek M., Puchalska M. and Jeżowska-Bojczuk M., New copper(I) complexes bearing lomefloxacin motif: Spectroscopic properties, in vitro cytotoxicity and interactions with DNA and human serum albumin, *J. Inorg. Biochem.* 165, 25 (2016).
- [30] G.G.Mohamed, Abd El-Halim H.F., El-Dessouky M.M.I. and Mahmoud W.H., Synthesis and characterization of mixed ligand complexes of lomefloxacin drug and glycine with transition metals. Antibacterial, antifungal and cytotoxicity studies, *J. Mol. Struct.* 2011, 999, 29.
- [31] W. Hanna, M. Moawad, *Trans. Met. Chem.* 2001, 26, 644.
- [32] J. Iqbal, S. Tirmizi, F. Watto, M. Inran, M.H. Watto, S. Sharfuddin, S. Latif, *Turk. J. Biol.* 2006, 30, 1.
- [33] P. Fernandes, Sousa L., Cunha-Silva L., Ferreira M., de Castro B., Pereira E.F., Feio M.J and Gameiro P., Synthesis, characterization and antibacterial studies of a copper(II) lomefloxacin ternary complex, *J. Inorg. Biochem.* 2014, 21, 131.
- [34] Z, aldefly, Z. Alshamkhani, M. Al-assadi, 2-hydroxybenzylidene-4-(4-SubstitutedPhenyl)-2-amino Thiazole and Their Pt (II) Complexes: Synthesis, Characterization and Biological Study, *EJCHEM*, 2019, 62, 4. DOI: 10.21608/ejchem.2019.10039.1661
- [35] W. H. El Shwiniy , S. A. Sadeek, Synthesis, Spectroscopic, Thermal Analyses and Biological Activity Evaluation of New Zirconium(IV) Solid Complexes with Bidentate Lomefloxacin, *EJCHEM*, 2018, 61, 27. DOI: 10.21608/ejchem.2018.3682.1323